POLITECNICO DI TORINO
Repository ISTITUZIONALE

Experimental evaluation of a fully recyclable thermoplastic composite

Terms of use:

Publisher copyright

(Article begins on next page)

23 September 2024

EXPERIMENTAL EVALUATION OF A FULLY RECYCLABLE THERMOPLASTIC COMPOSITE

S. Boria[1], A. Scattina[2], G. Belingardi[2]

[1]School of Science and Technology, University of Camerino
9 Madonna delle Carceri, Camerino, Italy
Email: simonetta.boria@unicam.it
[2]Department of Mechanical and Aerospace Engineering, Politecnico di Torino
24 Duca degli Abruzzi, Torino, Italy
Email: alessandro.scattina@polito.it, giovanni.belingardi@polito.it

Keywords: Lightweight design, Thermoplastic composite, Mechanical characteristics, Crashworthiness

ABSTRACT

For several years the application of composite materials with continuous fiber were limited to those with thermosetting matrix. Indeed, in recent years, there is a growing interest in composites with thermoplastic matrix thanks to the considerable advantages in terms of recyclability, and the reduction in weight and in production costs. In the automotive sector, increasingly stringent requirements for reduced emissions of CO_2, the maximum return on capital investment and the increase in plastic recycling and reuse, are some of the most important problems that directly influence the development of new materials. The thermoplastic composites appear to be the right alternative to the materials currently used for vehicles. They can replace not only the not structural parts (such as the interiors), but also the structural components located in areas potentially subject to impacts.

This paper presents the results of an experimental campaign made on a full thermoplastic composite, where both the reinforcement and the matrix are made in thermoplastic. The target is to know the mechanical properties in order to design an energy absorber with this new material. Initially, tensile, compression, bending and shear tests were made according to standards to obtain the mechanical characteristics. Subsequently, static and dynamic tests on thin-walled cylindrical tubes subjected to axial load were made in order to assess the energy absorption capacity varying the project parameters. The data were recorded and analyzed in terms of load-displacement curves, specific energy absorption (SEA), crush force efficiency (CFE), stroke efficiency (SE) and crushing stress. Comparing the new material to a common thermosets composite, different values of SEA are evident; fully thermoplastic composites are 3/4 times lower in energy absorption capacity. Nevertheless, taking into account the other favorable characteristic (such as full recyclability and shorter processing times) this fully thermoplastic material continues to be interesting for lightweight design. From the point of view of the energy absorption its spring back behavior offers some advantages respect to thermoset and conventional materials that tend to shatter and to buckle in the event of impact, respectively.

KEYWORDS: thermoplastic composite, experimental evaluation, energy absorber

1 INTRODUCTION

Currently carbon fiber reinforced polymers (CFRP) are used in several industries with individual technological and economical challenges. Nevertheless, the material utilization for an optimized lightweight structure and cost efficient manufacturing processes are cross-industrial requirements to enable the breakthrough of CFRP in high volume structural applications [1]. Composites in general have been used in the aerospace sector for decades due to lightweight design requirements for increased flight performance, as well as reduced operating costs that usually balance the upfront investment in more expensive material and process technologies. Since the material performance is the key factor, mainly high-end woven prepreg systems are being used respect to continuous or

discontinuous filament composites [2]. The comparative situation for automotive applications is slightly different. Key drivers for lightweight design are much more the upcoming government regulations and society needs, which require more efficient cars for the near future, with reduced fuel consumption and emissions [3-5]. So far, composite technology has only been established for niche cars and the step to high-volume automotive applications is very high. Low-cost material systems have to be developed as well as specific structural concepts for car bodies and automated manufacturing technologies. Repair and recycling are other important topics to be considered. As a first step towards high-volume production of a composite cars, BMW started with the production of the model i3 and i8 and other manufactures like Audi and Daimler will follow soon. While BMW is using a full composite concept for the life module, others will focus on hybrid structures at the body-in-white or component level. During the design of a car, next to the concept of lightness and recyclability, the safety aspect must not be forgotten. Composite materials are able to fulfill such requirements, if properly designed and implemented [6-8]. Conventional CFRP use thermosetting resin, which hardens when heated during the cure. Generally this material requires some minutes and sometimes tenth of minutes to mold in the desired shape, depending on the selected manufacturing technology, in these conditions it may result not suitable as a material for mass-produced automobiles. Highly stressed load-bearing structures and crash components made of composites are designed to buckle on impact in order to absorb the energy of the impact and consequently to protect the vehicle's occupants in the event of a collision. However, these materials tend to chip into sharp-edged splinters during an impact. It is therefore necessary to find a way for the automotive industry to mass-produce a particularly class of lightweight materials that can absorb the energy in a collision without splintering. Moreover, the currently used composites made with a thermoset matrix, brings to components that cannot be easily recycled at the end of life. Therefore, significant steps forward are needed for efficiency improvements along the whole process chain and the material and process costs have to be cut down significantly.

A possible solution to these problems can be the development of a new class of materials designed for large-scale use in vehicle construction, such as composite materials where both the fiber and the matrix are made in thermoplastic. Not only they can be shredded, melted down and reused to produce high quality parts, but they have been found also to perform significantly well in crash tests [9, 10]. When reinforced with textile structures they can absorb the energy of a collision through viscoelastic deformation of the matrix material, without splintering. While thermosetting composites involve several stages of processing, thermoplastic ones requires just two steps (press molding and demolding). For these reasons, the thermoplastic composite enables highly efficient production. Moreover, the cost of the thermoplastic matrix material and the cost of its processing are up to 50% lower than the equivalent costs for thermoset structures. Compared with traditional metals, plastics and thermoset composites, the fiber reinforced thermoplastic composites may result lighter, tougher and stiffer, with reference to weight rated values, as well as more sustainable, because they can be easily recycled and repaired. Finally they can be produced in high volumes with low costs.

In this overview, the paper presents the results of an experimental analysis conducted on a new thermoplastic composite in order to evaluate its energy absorption capacity. In particular, a plain thermoplastic weave combined with a thermoplastic matrix is considered. Firstly, an experimental test campaign is carried out, in order to define the mechanical properties of this innovative material under different load conditions. In particular tensile, compression, bending and shear tests have been done in quasi static conditions. The results of these tests and the consequently obtained mechanical properties are presented and discussed. Starting from the information obtained in the first experimental tests, the energy absorption capacity of simple impact attenuators with circular section made with thermoplastic composite is analysed. As regards to the geometry, symmetrical axial tubes have been used to carry out much of the experimental work on the energy absorption of composite materials because they are easy to fabricate and close to the geometry of the actual crashworthy structures. Moreover such composite tubes can be easily designed for stable crushing, absorbing impact energy in a controlled manner. For this reason, the crushing sensitivity of thin-walled circular tubes to the wall thickness and to the resistant section under quasi-static and dynamic loading conditions are presented and discussed. The data were recorded and analysed in terms of load-displacement curves, specific energy absorption (SEA), crush force efficiency (CFE), stroke efficiency (SE) and crushing stress. The results obtained with the thermoplastic specimens were compared with those typical of a traditional thermoset material.

The failure mechanisms, obtained varying the geometric parameters and the boundary conditions, will be also presented and discussed.

2   MATERIAL

The material studied in this work is a sealable, co-extruded triple layer polypropylene (PP) tape. It was provided by Lankhorst Pure Composites [11]. It was produced via the patented PURE technology. The PURE tapes are co-extruded and consist of a highly oriented, high strength and high modulus core and a specially formulated skin on both sides. The core and the two skins are welded together in a compaction process using a hot-press or continuous belt press. The Fig. 1 shows schematically the processing step of PURE. This process of co-extrusion and tape welding has enormous advantages over conventional sealing processes because of the large sealing windows (130-180°C) without loss of material properties. PURE material has a high stiffness and low density; the combination of these two properties makes PURE an interesting option for automotive products. Moreover, PURE material has good properties in impact resistance showing a "soft" (safe) crash behavior. In impact situation PURE does not splinter, but fails in a more ductile manner. PURE tapes were used for weaving into thermoformable plain fabric processes, using PP fibers embedded in the same PP matrix, thus achieving a mono material concept that is fully recyclable. Table 1 reports the main mechanical properties for tape and sheet configuration according to the PURE technical data sheet.

In the present work, the PURE fabrics were consolidated using 53 layers into a 600x1200 mm sheet reaching a thickness of about 6.9 mm. The flat specimens, used for mechanical characterization, were obtained from this sheet with a waterjet cut. Such PP material exhibits only minimal water absorption and permeability. For this reason the waterjet cutter seems the best option to obtain the desired tolerance. As regards to the geometry, symmetrical axial tubes have been used to carry out much of the experimental work on the energy absorption of composite materials because they are easy to fabricate and close to the geometry of the actual crashworthy structures. Moreover such composite tubes can be easily designed for stable crushing, absorbing impact energy in a controlled manner [12]. The production of cylindrical specimens was done by Von Roll Deutschland GmbH, thanks to its experience with the production of tubes out of PURE.
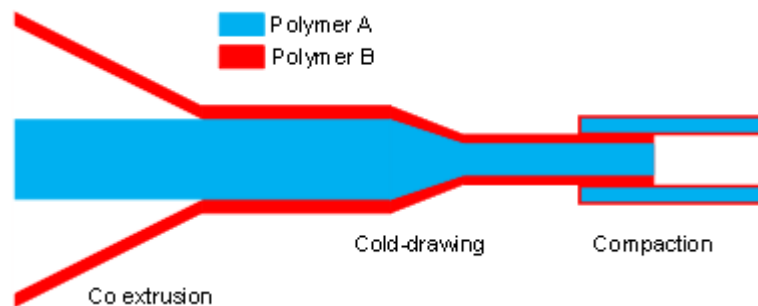

Fig. 1: Schematic processing step of PURE.

Table 1: Mechanical properties for PURE tape and sheet, from material data sheet.

PURE tape	Test method	Value	Unit
E-modulus	ISO 527	14	GPa
Tensile strength	ISO 527	500	MPa
Elongation	ISO 527	6	%
Shrinkage at 130°	ASTM D4974	<5.5	%
Sealing range		130-180	°C
PURE sheet	**Test method**	**Value**	**Unit**
Bulk density	ASTM D792	0.78	g/cm^3
Tensile modulus	ISO 527-4	5.5	GPa
Tensile strength	ISO 527-4	200	MPa
Tensile strain to failure	ISO 527-4	9	%
Flexural modulus	ISO 178	4.5-5.5	GPa
Charpy impact (FN)	ISO 179	(N, no break)	kJ/m^2
Charpy impact (EP notched type A)	ISO 179	(P) 140	kJ/m^2
Izod impact (FN)	ISO 180	(N, no break)	kJ/m^2
Izod impact (EP notched type A)	ISO 180	(P) 126	kJ/m^2
Instrumented falling dart impact (23°C) (2.2 mm, clamped, 20 mm striker)	ISO 6603-2	9.51 / 51.46	kN (peak) / J (at failure)
Heat deflection temperature (1820 kPa)	ASTM D648	95	°C
Coefficient of thermal expansion (-20°C to 100°C)	ASTM E228	23	$10^{-6}\ K^{-1}$
Coefficient of thermal conductivity (2.25 mm)	EN-ISO 12567-1	0.044	W/mK
Fire behaviour-burning rate (1.6 mm)	ISO 3795	29	mm/min

3   QUASI-STATIC TESTS FOR MECHANICAL CHARACTERIZATION

Initially standard coupon tests were performed in tension, compression, three points bending and shear according to ASTM Standards D3039, D3410, D790 and D5379, respectively. The tests were conducted in quasi static conditions with a servo-hydraulic Instron 8801 testing machine (Fig. 2). The tests were made at the Laboratory of the Department of Mechanical and Aerospace Engineering of the Politecnico di Torino. Such tests were carried out not only to verify the values of the data sheet for the material used, but also to use them for the development of finite element models able to reproduce the crushing phenomenon.

3.1 Tensile test

The specimens used for the tensile tests had a rectangular shape with the following dimensions: length 250 mm, width 20 mm with a thickness of 6.9 mm. The tensile tests were conducted in displacement control at three different crosshead speed (0.1, 5 and 100 mm/s) in order to evaluate the sensitivity of the material to the strain rate. The longitudinal strain of the specimens was measured by means of a dynamic extensometer Instron 2620-604 (Fig. 2). The tests were conducted up to the loss of load carrying capacity that, at the highest speed, resulted in the separation of the failed specimen in two parts (Fig. 3). The specimens after the test are shown in Fig. 3.
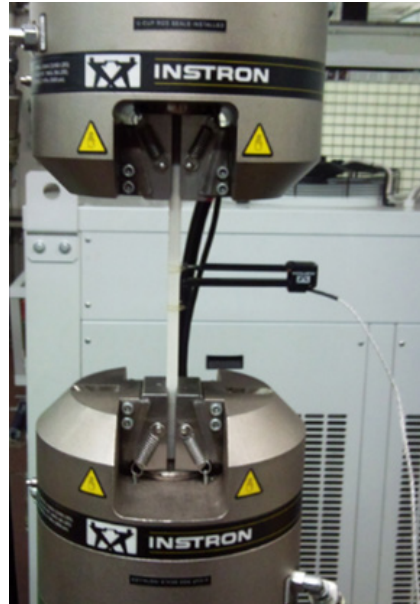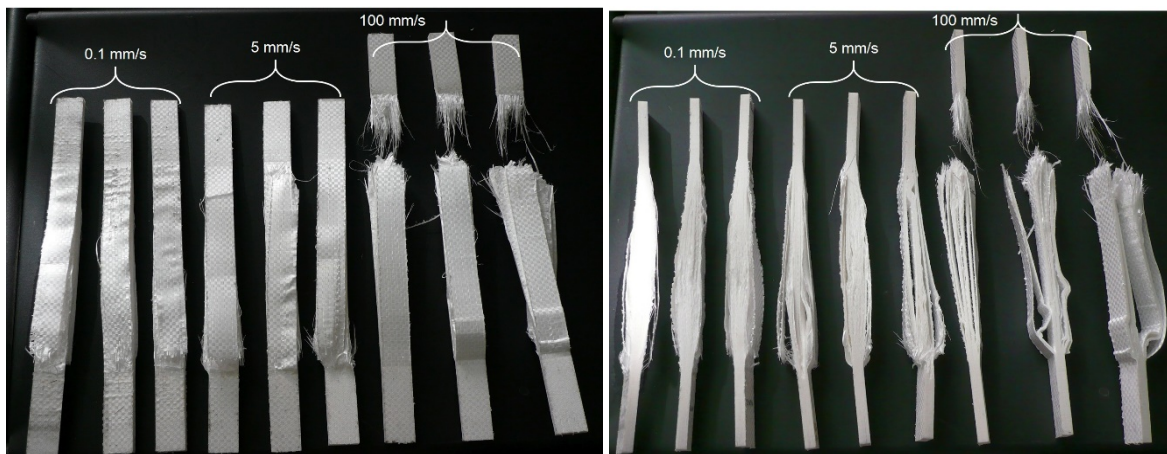
Fig. 2: The testing equipment.

Fig. 3: Specimens at the end of the tensile test, front view on the left, side view on the right.

The results of the tensile tests in terms of force-displacement and stress-strain diagrams are shown in Fig. 4. Fig. 5 shows the most important mechanical parameters as a function of the test speed. The main mechanical properties were calculated, as reported in Table 2. In particular the density ρ and the average values, calculated on the three speeds, of Young's modulus E, the tensile strength σ_u and the maximum elongation ε were evaluated. As it is possible to see, the results are relevantly influenced by the speed of the test. The elastic modulus and the tensile strength increase with the test speed, while the strain to failure decreases. Observing the curves of Fig. 4 it can be noticed that increasing the test speed, as it happens with plastic materials or metals, there is a certain hardening of the material. During the tensile test the first fracture happens on the fibers positioned on the external surface (polymer A on Fig. 1), then there is a sort of delamination and relaxation by the fibers positioned in the inner part (polymer B in Fig. 1). It seems that the specimen, before the test, is subjected to manufacturing residual stress. Increasing the test velocity, it is easier to see the delamination of the specimen. Obtained mechanical characteristics are not in complete accordance with those given by the material producer that were reported in Table 1.
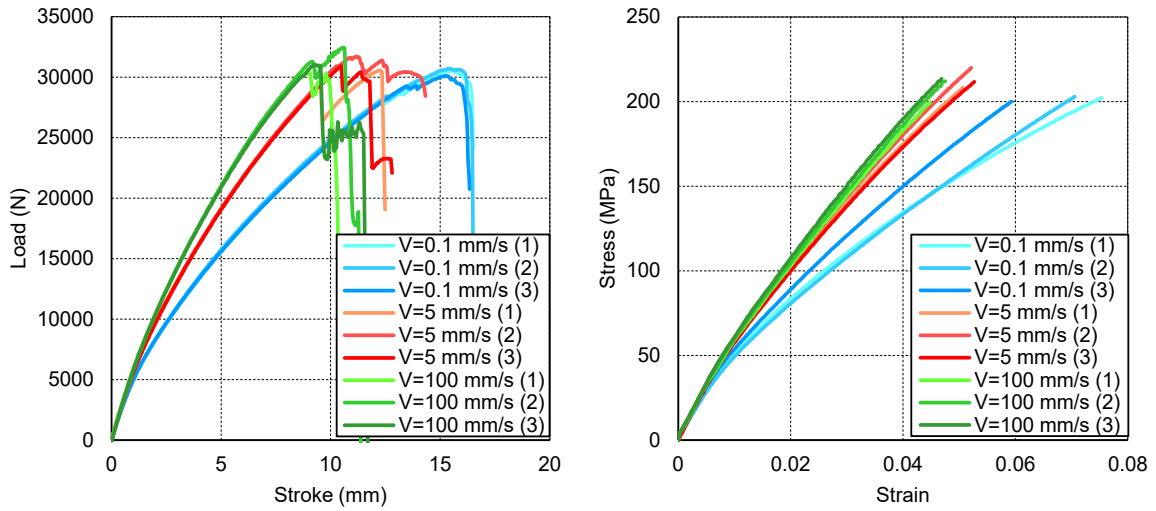
Fig. 4: Force-displacement (on the left) and stress-strain (only for the first linear part, on the right) diagrams for specimens under tensile test.
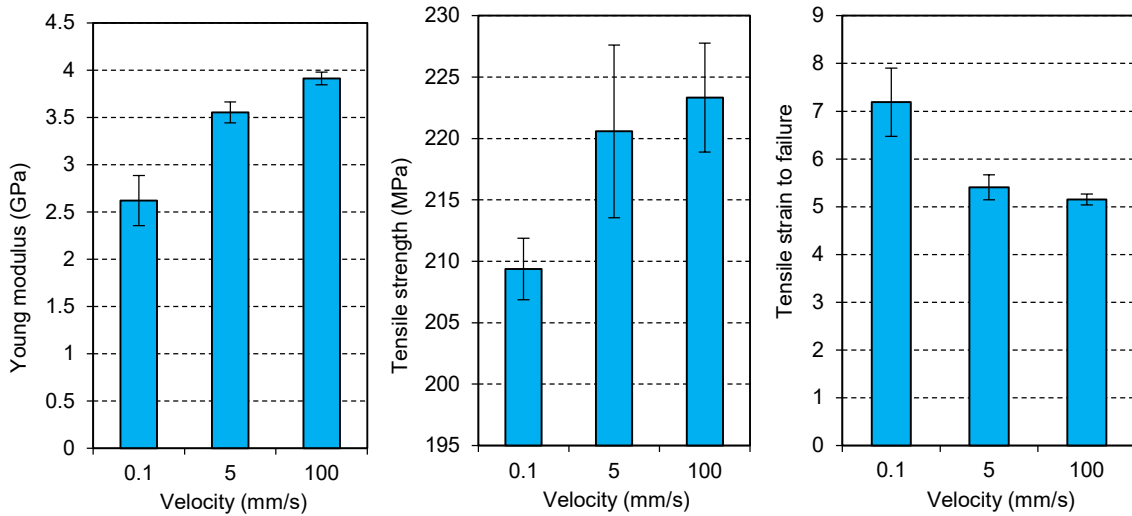

Fig. 5: Young's modulus, tensile strength and tensile strain to failure as a function of the speed test.

Table 2: Mechanical properties for the thermoplastic composite under tension.

Engineering constant	Units	Average value	Standard deviation
ρ	[g/cm^3]	0.78	-
E	[GPa]	3.4	0.10
σ_u	[MPa]	217.8	2.27
ε	[%]	5.9	0.31

3.2 Compression test

The specimens used for the compression test had rectangular shape with the following dimensions: length 150 mm, width 20 mm with a thickness of 6.9 mm. The span between the two grips was fixed to 50 mm. Compression tests were conducted at the crosshead speed of 2 mm/min. The tests were conducted up to loss of load (Fig. 6). The results of the tests in terms of force-displacement and stress-strain diagrams are shown in Fig. 7. The mechanical properties were calculated, as reported in Table 3. In particular the values of Young's modulus for compression E, the compressive strength σ_u and the compressive strain ε at maximum stress were evaluated. In the compression test the drop of the load is due to the delamination of the different layer with a consequent slip of one layer of fiber to another

one. There is a sort of packing of the fibers. Consequently the thickness of the specimen after the compression is higher than the initial one. After the test for some specimens, it is possible to note a little step in correspondence of the edge of the clamping device. This is due to higher compression stroke respect to others, that caused a packing of the fibers against the clamping grip. As expected the compressive elastic modulus results to be larger than the tensile one, while both the compressive strength and the maximum compressive strain result to be largely lower that the tensile ones.
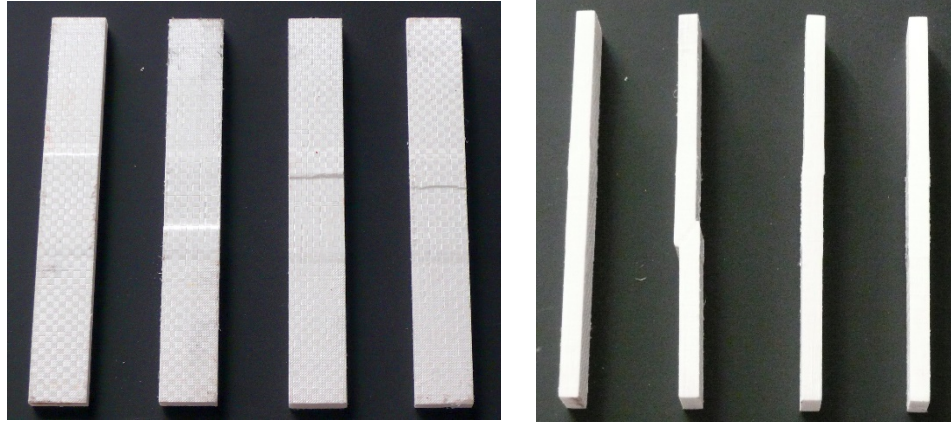

Fig. 6: Specimens at the end of the compression tests,
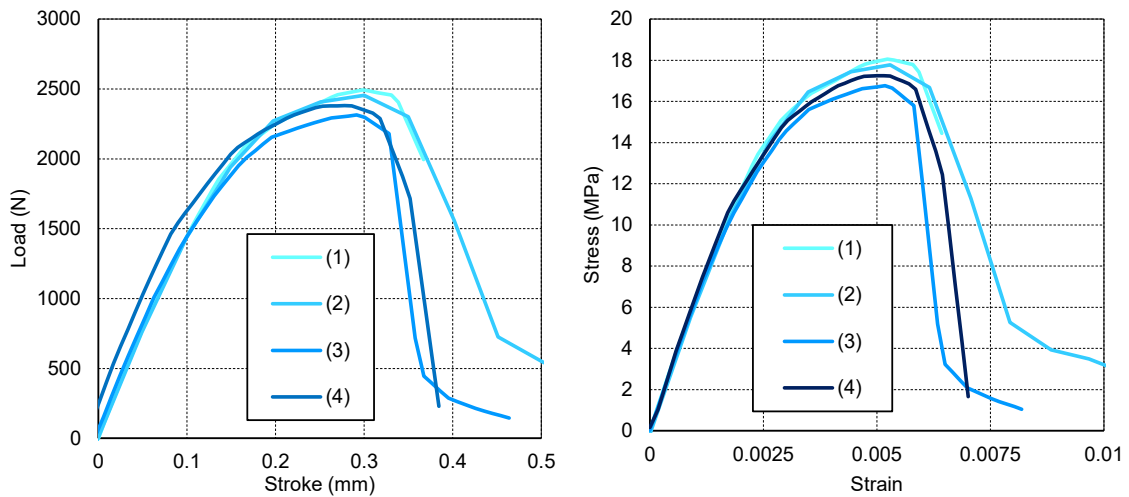on the left a front view, on the right a side view.

Fig. 7: Force-displacement (on the left) and stress-strain (on the right) diagrams
for specimens under compression test.

Table 3: Mechanical properties for the thermoplastic composite under compression.

Engineering constant		Average value	Standard deviation
E	[GPa]	5.1	0.21
σ_u	[MPa]	17.5	0.57
ε	[%]	0.52	0.01

3.3 Three points bending test

The specimens used for the three points bending tests, have the same geometry of that used for compression tests. Such tests were conducted at the crosshead speed of 2.85 mm/min, according to what is proposed by the standard (ASTM D790). For the same reason the span between the two supports was fixed to 107 mm. The tests were conducted up to loss of load (Fig. 8). The results of the tests, in terms of force-displacement and stress-strain diagrams, are shown in Fig. 10, while the

mechanical properties were calculated, as reported in Table 4. In particular the flexural modulus E and the flexural strength σ_u were evaluated. Observing the curves of Fig. 10 it is possible to note a first loss of the load, this is due to the detachment of the skin layer (polymer A on Fig. 1) near the central support, where the load is applied, as it is possible to see in the Fig.9, where the specimens after the tests are shown. Increasing the stroke, it is possible to note the curves of Fig. 10 a sharp drop of the load. This is due to the delamination, in the polymer B (as shown in Fig. 1) of a part of the specimen. The delamination, as it is possible to see in the Fig.9, is localized on one side of the specimen (left or right). Consequently, a reduction of the resistance bending module of the cross section is obtained. Subsequently the load maintains quite constant thanks to the ductile properties of the material.
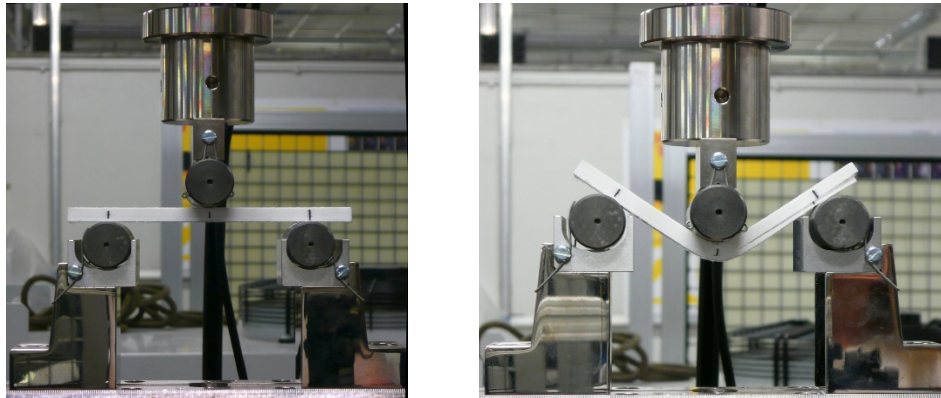

Fig. 8: The set-up of the testing machine before (on the left) and during (on the right) the three points bending tests.
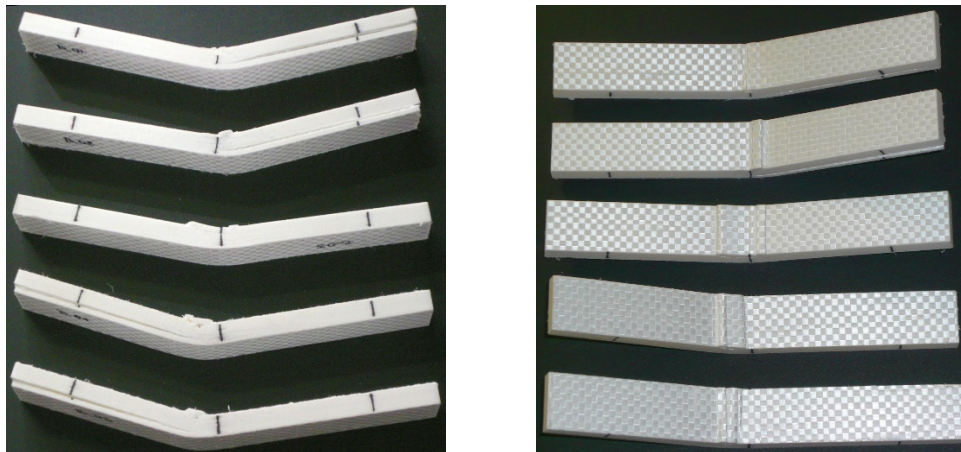

Fig. 9: Specimens at the end of the bending test: side view on the left, top view on the right.
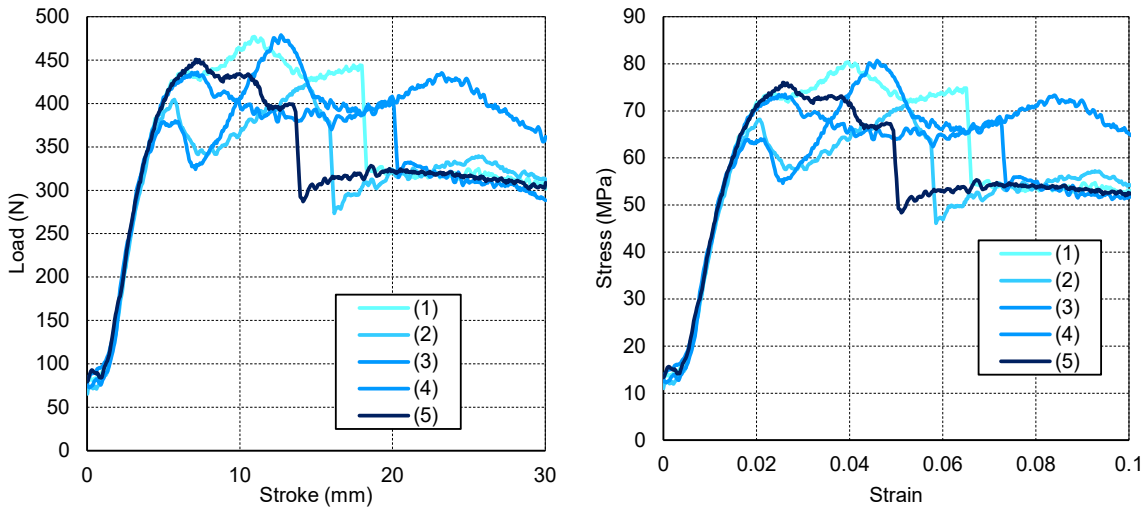
Fig. 10: Force-displacement (on the left) and stress-strain (on the right) diagrams
for specimens under three points bending test.

Table 4: Mechanical properties for the thermoplastic composite under bending.

Engineering constant		Average value	Standard deviation
E	[GPa]	4.7	0.11
σ_u	[MPa]	76.4	4.18

3.4 Shear

During the last decades, an intensive research effort has been devoted to the experimental identification of shear properties of orthotropic composite materials. Different shear test methods have been proposed [13], among which there is the Iosipescu shear test. It was firstly developed to measure the shear strength of metal rods [14] and has been studied extensively by the composite research community within the last 20 years, starting with the work of Walrath and Adams [15] in the early eighties. In this type of test the specimen has the shape of a rectangular beam of small dimensions, with symmetric V-notches at its center (Fig.11). A suitable fixture is used (Fig. 12 on the left) in order to transform the applied load into a shear loading, acting at the specimen minimum cross-section area, between the V-notches. The geometry of the V-notches is such that a quasi-uniform shear-stress distribution is produced at the center of the specimen [13]. The test was done at a controlled displacement rate of 2 mm/min up to the maximum displacement of the testing machine.

The force vs displacement and the mean stress vs strain curves are shown in Fig. 13. Table 5 summarizes the main mechanical characteristics calculated, such as the shear modulus G, the yield stress τ_y, the ultimate shear strain and the strength (ε_u and τ_u). None of the tests terminated with specimens failure. Examining the deformations on the specimen, a ductile slip and compaction of the fibers in the center of the notch can be observed (Fig. 12 on the right). This phenomenon explains the tendency to increase the load in the final part of the curves (Fig. 13 on the left).
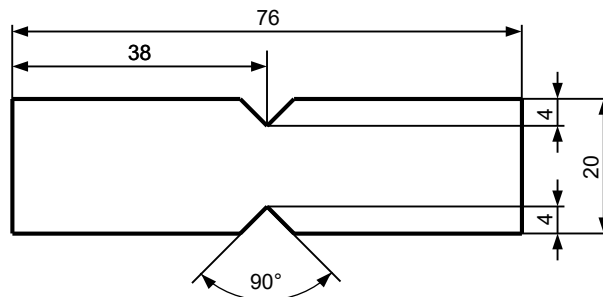

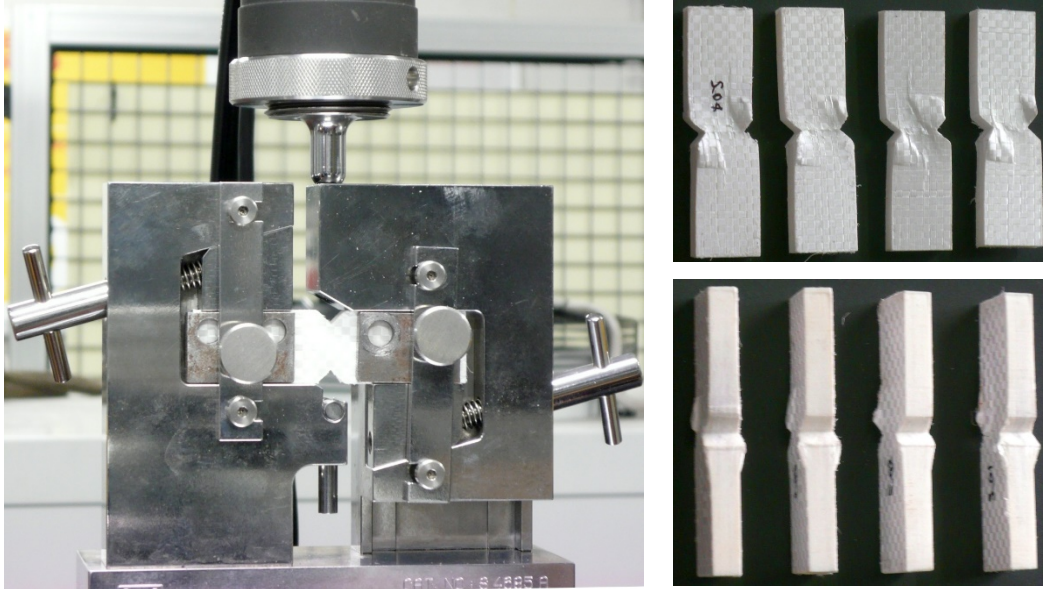Fig. 11: Geometry of the Iosipescu specimen.

Fig. 12: Specimen during the test (on the left) and at the end of the test (on the right).
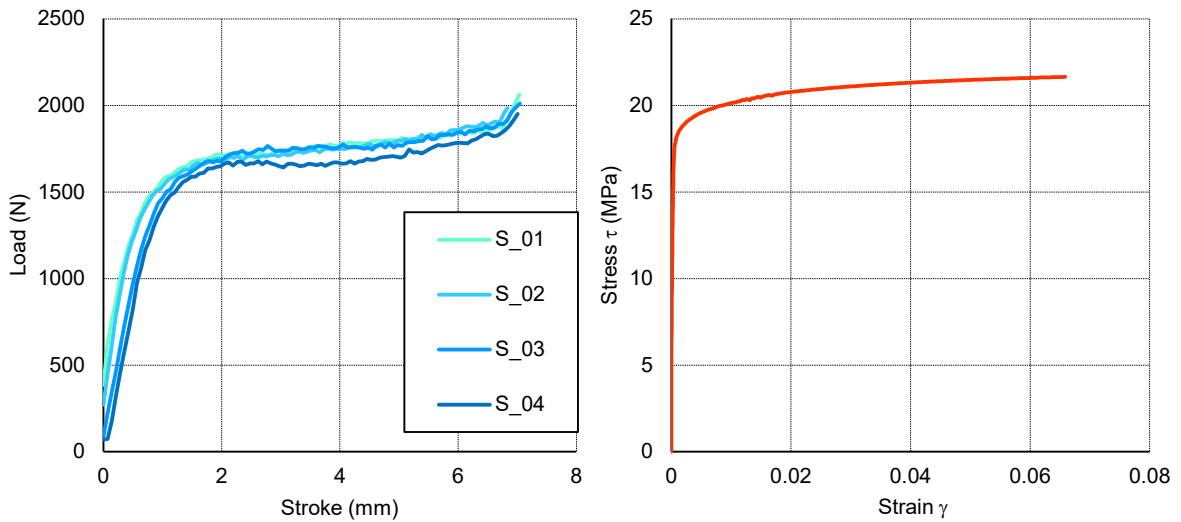

Fig. 13: Force vs displacement curves (for all the specimens tested)
and stress vs strain (mean value).

Table 5: Mechanical properties for the thermoplastic composite under shear.

G [GPa]	τ_y [MPa]	ε_u	τ_u [MPa]
11.15	16.03	0.065	21.64

4   CRUSHING TESTS: METHODOLOGIES AND MECHANISMS

Crush tests were carried out on tubular specimens with circular cross section in two loading conditions, namely quasi-static and impact ones. In quasi-static testing, the specimen is crushed at a low constant speed, whereas in the impact ones the crushing speed in much higher. Quasi-static tests may not be a true simulation of the actual crash condition, because in a real situation the structure is subjected to a progressive decrease in crushing speed, from an initial impact speed to final rest. Moreover many materials used in crashworthy structures are rate sensitive. This means that their energy absorption capability is dependent on the speed at which they are crushed. Therefore, the determination of materials as good energy absorbers after quasi-static tests does not ensure their satisfactory performance as crashworthy structures in the event of true crash. However, quasi-static

tests are used, initially, to study the failure mechanisms that take place during the crushing of the structures.

Circular cylindrical structures can deform in compression by at least four competing mechanisms [16]: tube inversion, progressive crushing, axisymmetric buckling and diamond-shape buckling (Fig. 14). Catastrophic failure modes are not of interest for the design of crashworthy structures, because they are characterized by a sudden increase in load to a peak. This value is then followed by a low post failure sustained load. Consequently, the magnitude of energy absorbed in those cases is much less and the peak load is too high to prevent injury to the passengers. Moreover, structures designed to react to loads produced by catastrophically failing energy absorbers are generally heavier than structures designed to react to loads produced by progressively failing energy absorbers [17]. Compressive crushing is the most observed failure mode for FRP composite tubes in compression [18]. It ensures high energy absorption associated to a large number of micro fractures that occur as the tube crushes. The energy dissipation results from the generation of fracture surface area, from friction between fragments and from plastic shear of the matrix. Metallic and polymeric cylindrical shells instead tend to absorb energy through the creation of a sequence of folds [19]. The ratio of tube wall thickness to tube radius is the dominant factor in determining whether axisymmetric buckling or diamond buckling will occur in both elastic and plastic buckling: thick isotropic tubes fail by axisymmetric buckling while thin-walled tubes fail by diamond one [20, 21]. For geometries close to transition values, the crushing behaviour can switch from one mode to another during a single test [22].
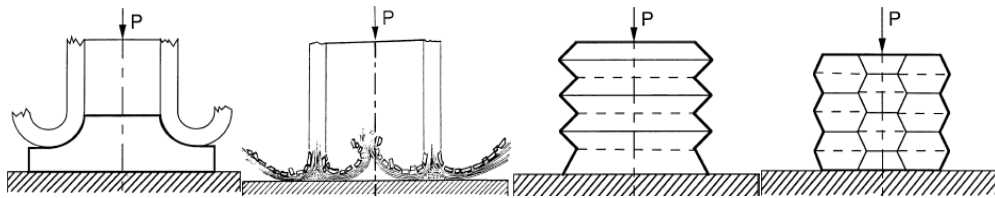

Fig. 14: Axial modes of collapse for cylinders (a) tube inversion, (b) progressive crushing, (c) axisymmetric buckling and (d) diamond buckling.

4.1 Quasi-static tests for energy absorption capacity

In order to analyse the energy absorption capability of the examined material, considering a possible use as structural components, static tests on thin-walled cylindrical tubes were carried out. The geometric characteristics of the specimens are summarized in Table 6. The structures differ each other for the inner diameter D_i, the wall thickness t, while maintaining a constant height of 200 mm. The different specimens were identified by a code defined as D_i_t, as reported in Table 6.

The specimens were submitted to quasi-static tests characterized by a speed of 5 mm/s and a maximum axial crushing of 100 mm (Fig. 15). Tests have been done with the same machine, the same equipment and the same general conditions as described in the previous paragraphs.

Table 6: Geometric characteristics of the tubular specimens.

# Specimen	Code	Inner diameter D_i [mm]	Wall thickness t [mm]
1	50_2	50	2
2	50_3	50	3
3	50_4	50	4
4	80_2	80	2
5	80_3	80	3
6	80_4	80	4
7	100_2	100	2
8	100_3	100	3
9	100_4	100	4

The load-displacement and the energy-displacement diagrams, for all the tested specimens, are shown in Fig. 16. Table 7 reports some parameters characterizing the crush resistance under static loading evaluated with the experimental tests. In particular, the values of the average crushing stress σ_{av}, the total absorbed energy E_{abs}, the specific energy absorbed (SEA), the crush force efficiency (CFE) and the stroke efficiency (SE) were calculated. Being in such cases the section constant during the crushing, σ_{av} is the ratio between the average crushing force F_{av} and the specimen cross sectional area A, that is:

$$\sigma_{av} = \frac{F_{av}}{A} \qquad (1)$$

The total absorbed energy E_{abs} is the amount of energy that the specimen absorbed during the entire axial crushing. The value is calculated considering the area under the load vs displacement curve, that is:

$$E_{abs} = \int_{0}^{\delta} F(h)dh \qquad (2)$$

where δ represents the total crushing.
The SEA is the energy absorbed per unit of mass of the crushed structure, obtained by:

$$SEA = \frac{E_{abs}}{\rho A \delta} \qquad (3)$$

being ρ the density of the material. Therefore the SEA is not an intrinsic material property. It depends not only on the material properties, but also on several other parameters, especially the specimen geometry. Two specimens made of the same material but with different geometries can collapse in very distinct ways and, as a consequence, can achieve very different values of SEA. The SEA allows comparing the energy absorption capabilities of two different materials and geometries when the weight is an important parameter of project. High values indicate lightweight crash absorbers.
The CFE is defined as the ratio between the mean load and the maximum peak load F_{peak}, that is:

$$CFE = \frac{F_{av}}{F_{peak}} \qquad (4)$$

If the crushing efficiency is equal to one the behavior is called as perfectly plastic, the load versus displacement diagram has a rectangular shape and the structure is considered an ideal attenuator. The effective crush length divided by the total tube length L is indicated with SE :

$$SE = \frac{\delta}{L} \qquad (5)$$

In the ideal case, an energy absorber is also as compact as possible, with a length L equal to the useful stroke length δ; in practice, the stroke efficiency is less than unity. In summary, crashworthiness is maximized by using an energy absorber of high crush force efficiency and of high stroke efficiency.

The considered PURE material under axial loading shows a "soft" crash behavior. It does not splinter, but fails in a more ductile manner. Examining in detail the deformation during the crush tests (Fig. 17), the main behavior is a non-regular folding. For the lowest diameter (D_i=50 mm) after a certain package of the material (around 50 mm of stroke) the deformation mechanism changed from folding to bending, consequently the process became instable. This phenomenon was encountered again although in a different way while increasing the diameter. In particular, with the highest wall thickness, in some cases, the deformation mechanism changed from axi-symmetric to diamond folding [23]. The most regular behavior in terms of energy absorption was obtained with the smaller diameter and the intermediate thickness (D_i=50 mm and t=3 mm).
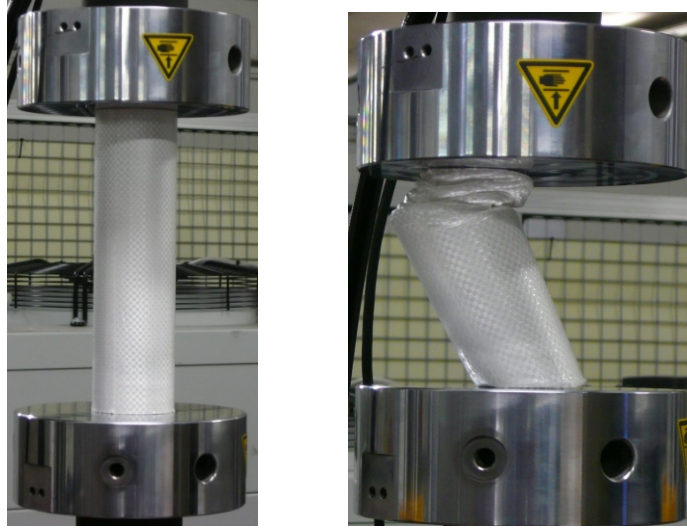
Fig. 15: Specimen under quasi-static compression
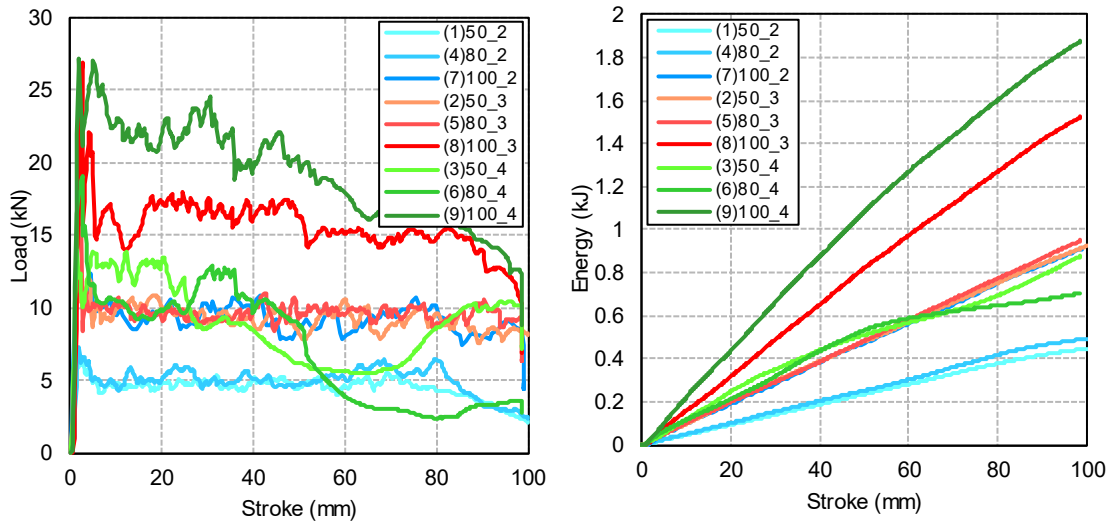before (on the left) and during (on the right) the test.

Fig. 16: Load (on the left) and energy absorbed (on the left) versus stroke displacement for all tested tubes.

Table 7: Static results for the tested specimens.

# Specimen	Code	Average crushing stress σ_{av} [MPa]	Absorbed energy E_{abs} [kJ]	SEA [kJ/kg]	CFE	SE
1	50_2	13.64	0.45	17.52	0.71	0.49
2	50_3	18.49	0.93	23.77	0.73	0.50
3	50_4	12.84	0.88	16.84	0.62	0.49
4	80_2	9.56	0.49	12.28	0.67	0.50
5	80_3	11.51	0.95	15.82	0.49	0.49
6	80_4	6.34	0.71	8.69	0.35	0.49
7	100_2	9.34	0.91	18.48	0.34	0.49
8	100_3	15.05	1.52	20.42	0.55	0.49
9	100_4	13.82	1.88	18.69	0.66	0.49

Fig. 17: Specimens at the end of the compression test.
From top to down the diameter increases, from left to right the wall thickness increases.

Fig. 18 shows how the average crushing stress and the specific energy absorption (SEA) vary with the thickness/inner diameter ratio (t/D_i). Even if the data are quite scattered, it is clear that increasing the wall thickness or decreasing the inside diameter the values increase almost linearly. Such trend was also observed for thin-walled CFRP composite structures under axial loading [24]. If the data inherent to the geometry 80_4 is not considered in the diagram, not only because it appears as an anomalous result but also because this is explained (as it is well visible in Fig 17) by a completely different collapse mode i.e. a global bending collapse, it seems more reasonable to interpolate the results with a polynomial regression of the second order (Fig.19). In this way a better fitting of the data can be obtained. The interpolation curve, in his latter case, put in evidence the presence of a maximum for a (t/D_i) ratio approximately equal to 0.06.
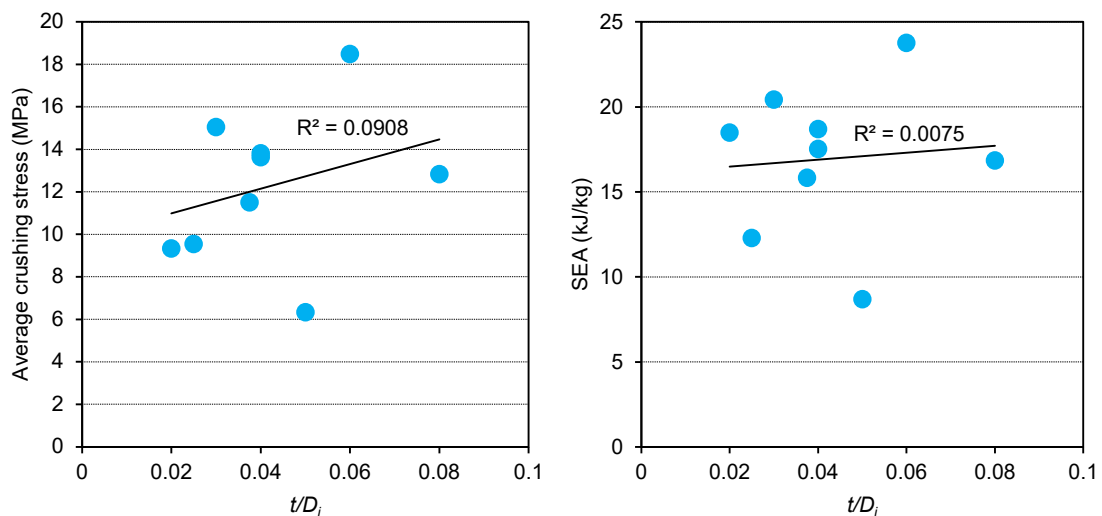

Fig. 18: Average crushing stress and SEA varying the ratio t/D_i taking into account all values. The data are interpolated with a linear curve.
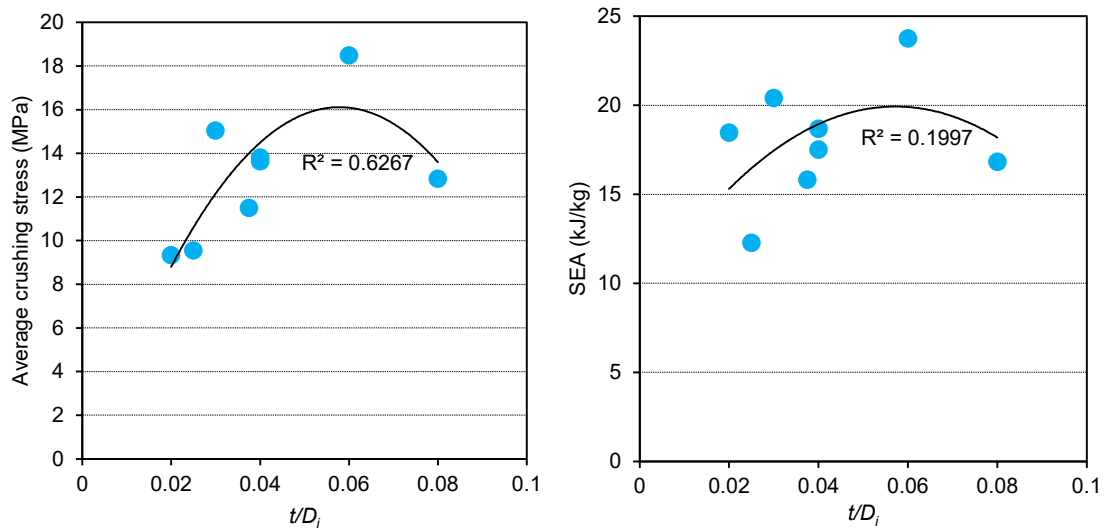
Fig. 19: Average crushing stress and SEA varying the ratio t/D_i removing the 80_4 values. The data are interpolated with a second order curve.

4.2 Dynamic tests for energy absorption capacity

The dynamic experimental tests were done using a drop weight machine [24] at the Picchio Spa laboratory (Fig. 20). The mass used for all tests were 301 kg; Table 8 reports the specific impact velocity used for the respective specimen. During the tests, each tube was bound to the tower base by an internally hollow steel support of 10 mm in height, in order to fix the tube avoiding sudden and uncontrolled slips in the first impact phase. The impact accelerations and the velocity were acquired by a tri-axial accelerometer with ±180 g full scale and a photocell, respectively. The accelerometer was placed on the impact mass. Moreover, a high speed camera with a sampling of 1000 frames/s was used. The deformation process registered by camera is, in fact, necessary to analyze in detail the energy absorption capacity of each tube.
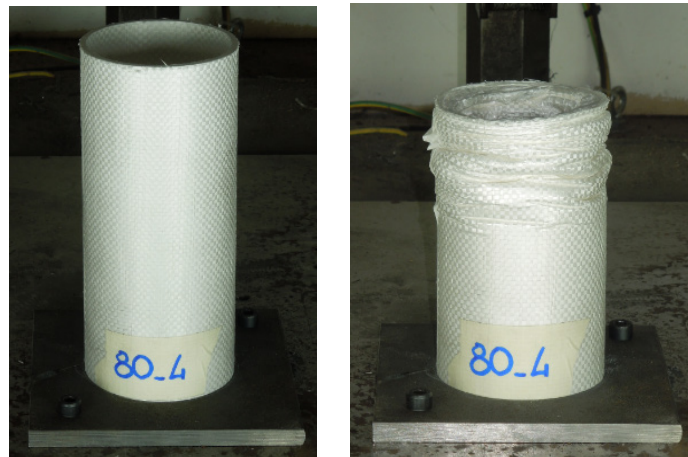

Fig. 20: Specimen under dynamic compression
before (on the left) and after (on the right) the test.

The load-displacement and the energy variation chart, for all the tested specimens, are shown in Fig. 21. It is possible to note a remarkable difference in terms of absorbed energy for same cases; this is due to the fact that for only specimens with 100 mm in internal diameter higher levels of kinetic energy were used during test. Table 8 reports some parameters characterizing the crush resistance under dynamic loading evaluated with the experimental data. In particular, the values of the average crushing stress, the absorbed energy, the specific energy absorbed (SEA), the crush force efficiency

(CFE) and the stroke efficiency (SE) were calculated as for the quasi-static tests.
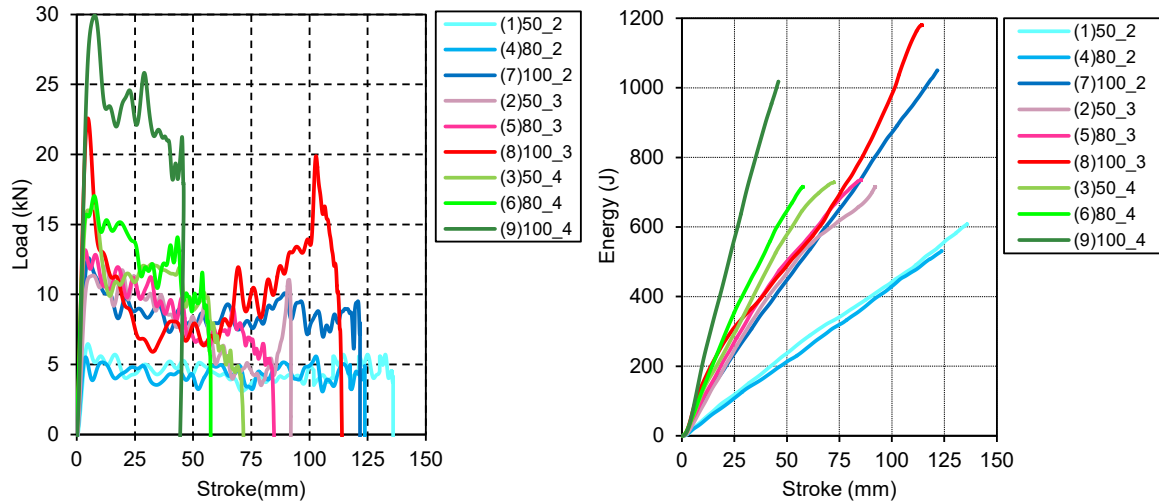

Fig. 21: Load (on the right) and crushing stress (on the left)
versus displacement for all tested tubes.

Table 8: Dynamic results for the tested specimens

# Specimen	Code	Impact velocity [m/s]	Average crushing stress σ_{av} [MPa]	Absorbed energy E_{abs} [kJ]	SEA [kJ/kg]	CFE	SE
1	50_2	2.01	13.66	0.61	17.56	0.69	0.68
2	50_3	2.19	14.56	0.72	19.94	0.61	0.46
3	50_4	2.20	9.62	0.73	18.99	0.40	0.36
4	80_2	1.88	8.35	0.53	10.68	0.77	0.62
5	80_3	2.22	7.91	0.74	14.12	0.47	0.43
6	80_4	2.19	9.85	0.72	15.09	0.61	0.29
7	100_2	2.64	13.32	1.05	17.26	0.68	0.61
8	100_3	2.80	9.47	1.18	13.64	0.41	0.57
9	100_4	2.60	16.26	1.02	21.72	0.71	0.23

Also from the dynamic point of view such PURE structures under axial loading shows a ductile crash behavior, combining axisymmetric buckling with diamond one and bending, although with lesser extent compared to the static case (Fig. 22). The Fig. 23 shows how the average crushing stress and the specific energy absorption (SEA) vary with the thickness/inner diameter ratio. Also in this case, an interpolation of the experimental results with a polynomial regression of the second order allows to obtain better fitting of the data (Fig. 23). For the average crushing stress it is evident a more constant behavior, varying t/D_i, than with the static loading condition; moreover also the SEA in dynamic conditions tends to increase even if with a lower slope.
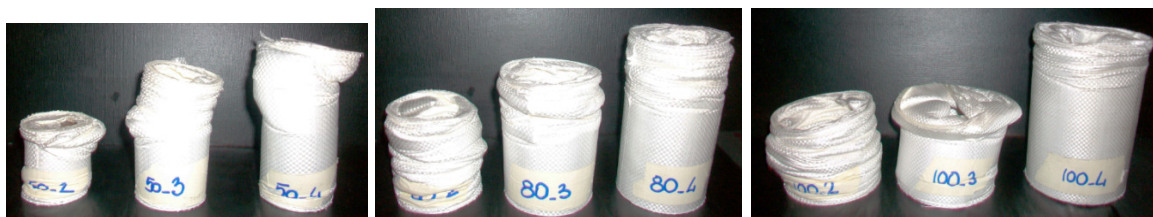

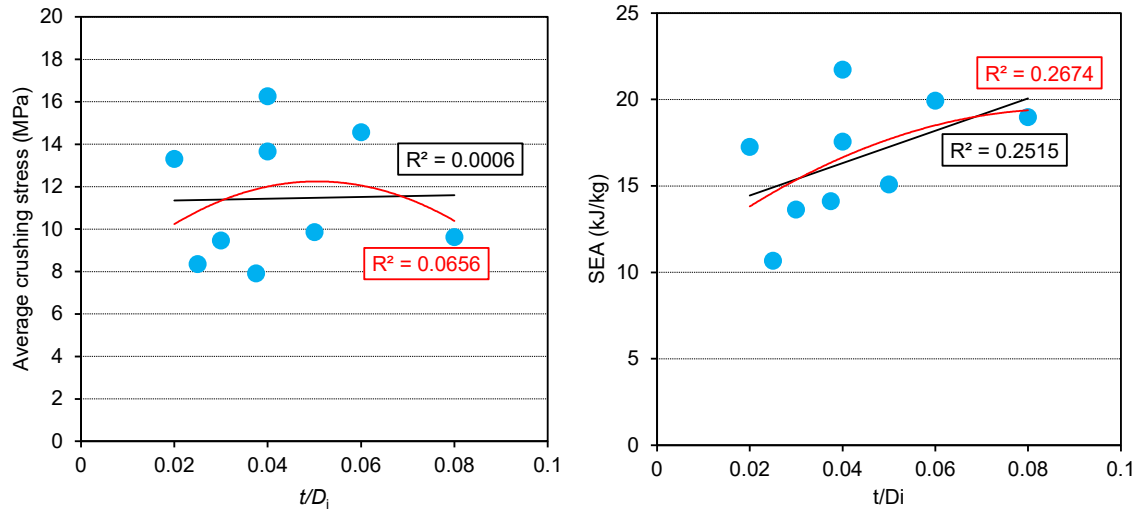Fig. 22: Specimens at the end of the dynamic compression test.

Fig. 23: Average crushing stress and SEA varying the ratio t/D_i interpolated with a linear regression (black line) and with a polynomial regression (red line)

5 FURTHER ANALYSIS AND DISCUSSION OF THE CRUSHING TESTS RESULTS

All the tested tubes absorbed the crushing energy through a plastic buckling failure mode. This is due to the nature of the thermoplastic polymers, different from the thermosetting ones. In the thermoplastic polymers the general structure is a flexible linear chain, while for thermosetting ones it is a rigid three dimensional network. The thermoplastic polymers work with a plastic, ductile behavior; no more brittle fracture can be observed as for the case of FRP composites. Thermoplastic polymers are produced at elevated temperatures, cooled and then reheated and reformed into a different shape without change of the basic structure or properties during processing. At low strain rates, viscoelasticity properties of the polymer control the creep properties. At impact loadings there is not enough time for the chains to move and this causes plastic deformation.

Comparison between the tubes tested statically and those subjected to dynamic compression shows a similar failure mode, even if the bending phenomenon is less evident during compression at higher speed. Fig. 24 shows three diagrams where the load vs displacement curves of the quasi-static tests are superimposed: each diagram has a constant value of the wall thickness while the three curves are for the three different values of the inner diameter. Similarly Fig. 25 shows three diagrams where the inner diameter is characterizing each diagram while the three curves are for the three different values of the wall thickness. Analyzing the static behavior, it is evident that the absorbed energy and the average load tend to rise sharply when the diameter becomes 100 mm; while between 50 and 80 mm no great change is found (Fig. 24). Moreover, while there is an evident increase of load passing from 2 mm to 3 mm, a change of the same amplitude cannot be seen while passing from 3 mm to 4 mm (Fig. 25). This is due to the transition from the buckling mode to the bending deformation, responsible of a lower energy absorption capacity.
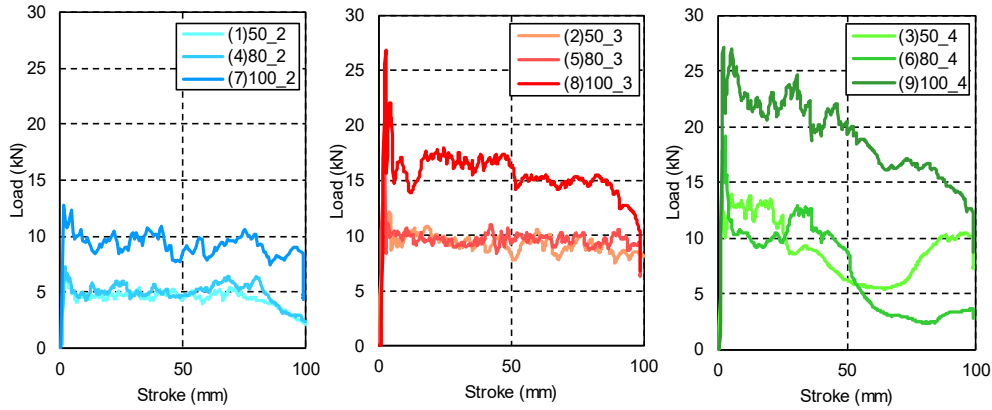
Fig. 24: Static load trend varying internal diameter for each wall thickness.
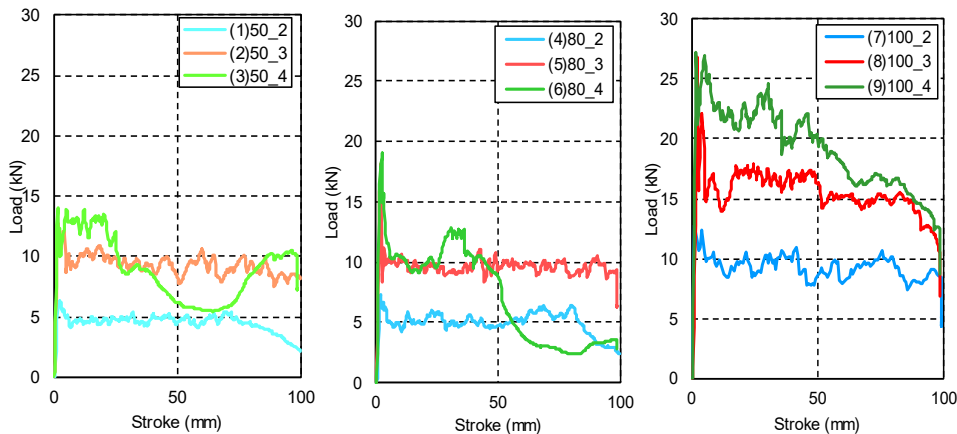

Fig. 25: Static load trend varying wall thickness for each internal diameter.

All the values of the SEA obtained considering all the possible combination of thickness and inner diameter evaluated, have been interpolated with a quadratic surface. The interpolation has been done both for the static and the dynamic tests. The results of the interpolation have been shown in Fig. 26, for the static case, and in Fig. 27 for the dynamic one. The interpolation is excellent for the static analysis, indeed the value of determination coefficient R^2 is equal to 0.92. The correlation of the experimental data with the surface for the dynamic case is lower, being the R^2 value equal to 0.75. As it is possible to see in the figures, the type of surface is different in the two cases. While for the static case the response surface is a hyperbolic paraboloid with a saddle point, in the dynamic conditions the data can be interpolated with an elliptical paraboloid with a concavity upwards. In the static case, the maximum values of the SEA are concentrated for the intermediate value of the thickness, and for the minimum or the maximum value of the inner diameter. For the dynamic case, to obtain the maximum SEA values, the diameter values follow the same rule as before, whereas the thickness should be maximized. This difference can be attributed to the final deformation of the tube with highest wall thickness value; under dynamic loading conditions, minor bending phenomena are evident and therefore higher SEA values can be recorded respect to the static case. From the interpolation surfaces the maximum SEA values have been extracted for both loading conditions, as shown in Table 9.
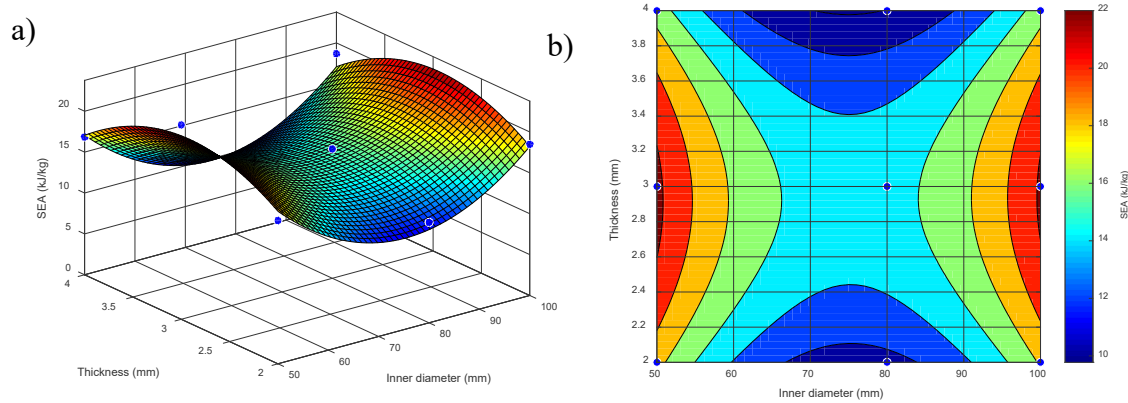
Fig. 26: Interpolation of the static SEA results: a) surface and b) contour plot.
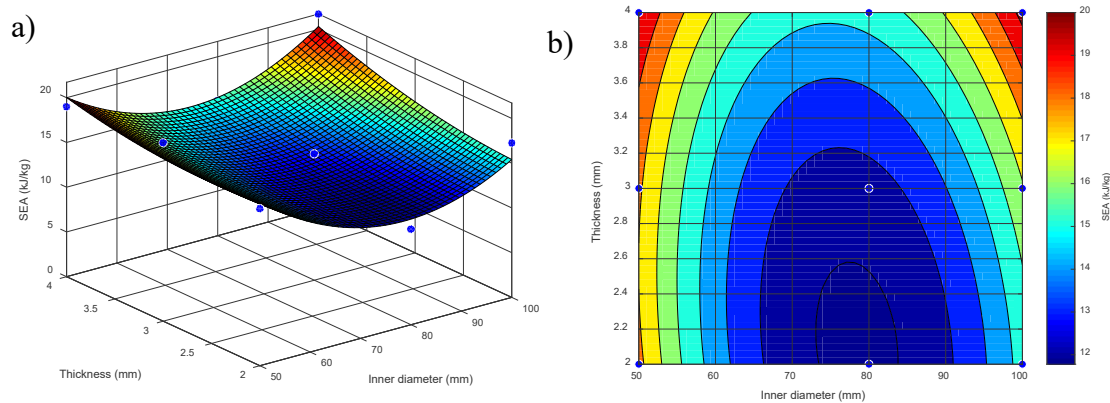

Fig. 27: Interpolation of the dynamic SEA results: a) surface and b) contour plot.

Table 9: Maximum SEA values and optimized parameters obtained with the interpolation

	STATIC	DYNAMIC
SEA max (kJ/kg)	22.46	20.32
Inner diameter (mm)	50	100
Thickness (mm)	2.91	4

Fig. 28 shows how the specific energy absorption varies with the thickness/inner diameter ratio. Although data are quite scattered, it is clear that increasing the wall thickness or decreasing the inside diameter the SEA tends to increase up to a certain value and then decreases. As it is possible to observe in such analysis, there is no so remarkable difference in energy absorption capability between static and dynamic load conditions. Upon reviewing the literature, there seems to be a lack of consensus about the influence of test speed on the energy absorption of FRP composite structures [25-32]. In most cases, it was reported a relevant decrease (up to 35%) in energy absorption with increasing test speed. In other works, the specific energy seems to be independent of crushing speed or even a change of tendency was found [17]. The rate at which the structure is loaded has an effect on the material's behavior. Also the structural response of the target is influenced. The strain energy absorbing capabilities of the fibers and the geometrical configuration of the target are very important factors that determine the impact resistance of composites at low speeds, while they become less important at very high strain rates since the structure responds in a local mode. What is important is the magnitude of the energy dissipated in delamination, debonding and fiber pull out.

Taking into account such aspects and analyzing the results also in terms of crush force efficiency and crushing stress, it is clearly evident that to improve the energy absorption capacity of the

component it is useful to adopt geometries with t/D_i values between 0.04 and 0.06. To avoid no regular deformation and instable behaviour, the values of the geometric parameters should be carefully defined.
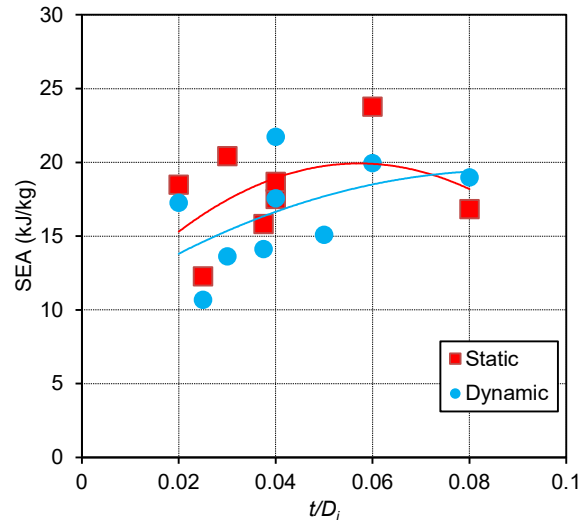

Fig. 28: SEA values varying wall thickness/diameter ratio.

It is also of interest to make a comparison between of the considered thermoplastic composite and a traditional thermosetting one. Different values of SEA are evident; whereas CFRP tubes have the capacity to absorb energy with mean values of SEA between 50 and 70 kJ/kg [24], depending on the strain rate condition, specific energy absorption for fully thermoplastic ones are 3/4 times lower. This difference is mainly due to the very different mechanical characteristic of the two types of considered fibers. Nevertheless, taking into account the other favorable characteristic (such as full recyclability and shorter processing times) this fully thermoplastic material continues to be interesting for lightweight design. From the point of view of the energy absorption its ductile behavior offers some advantage.

6 CONCLUSIONS

The paper describes the experimental campaign carried out on a new thermoplastic composite, where both the fibres and the matrix are made with thermoplastic. The experimental tests were made in order to characterize the material from the mechanical point of view and to verify its ability to absorb energy when used to make thin-walled cylindrical tubes. Tensile, compression, three points bending and shear tests were conducted, under quasi-static conditions, according to ASTM Standard in order to get the base data for its mechanical characteristics. Moreover, axial crushing experimental tests on simple cylindrical structures were done, under both static and dynamic conditions. In this configuration the sensibility of the wall thickness and of the dimension of the tubes was investigated by means of a full experimental plan.

As regards the failure mechanisms of considered thermoplastic tubular structures, for some aspects the crushing behaviour is similar to conventional metallic materials, whereas, for some others aspects, typical composite crushing behaviour is observed. As for metallic structures under axial loading, a sequence of localised plastic hinges according to the concertina or diamond deformation modes can be observed. Differently from them the force-shortening characteristic does not present a clear sequence of peaks and valleys. An almost constant crushing strength throughout the deformation process it is evident, as it happens for composite structures, although in the examined case this does not involve a brittle failure. For some tubular specimens, after a certain compression stroke, it is possible to observe a loss of load bearing capacity due to a change in the deformation type, which passes from folding to bending. In any case the crushing behaviour of such new material results to be quite interesting because, by choosing in right way the combination of the thickness and the diameter of the tube, it is possible to obtain a regular folding behaviour accompanied by a nearly flat load-displacement diagram

with a consequently high and regular energy absorption. For these reasons this material shows good opportunity to be used as lightweight material in automotive applications.

The recorded data were analysed in terms of load-displacement curves, specific energy absorption (SEA), crush force efficiency (CFE), stroke efficiency (SE) and crushing mean stress. Analysis of the results clearly puts in evidence that to improve the energy absorption capacity of the component it is useful to increase the thickness of the laminate and to decrease the inside diameter. To avoid no regular deformation and instable behaviour the value of the diameter should be carefully defined. Results obtained from the dynamic impact tests are substantially confirming what we have seen from the quasi-static crushing tests. The two SEA diagrams are well superimposing.

Finally, between the different examined solutions it seems reasonable to define as the best case the geometries with t/D_i values between 0.04 and 0.06. For this solutions, the trend of the load curve during crushing is very regular without oscillations, such as an ideal energy absorber.

REFERENCES

[1] McKinsey & Company, Advanced Industries, Lightweight heavy impact, 2012.

[2] E. Mahdi, A.S.M. Hamouda, A.S. Mokhtar, D.L. Majid, Many aspects to improve damage tolerance of collapsible composite energy absorber devices, *Composite Structures*, 67:175-187, 2005.

[3] P. Mock, European vehicle market statistics pocketbook 2013, International Council on Clean Transportation, Berlin, Germany, 2013.

[4] C. Koffler, K. Rohde-Brandenburger, On the calculation of fuel savings through lightweight design in automotive life cycle assessments, *The International Journal of Life Cycle Assessment*, 15: 128-135, 2010.

[5] G. Belingardi, G. Chiandussi, Vehicle crashworthiness design – general principles and potentialities of composite material structures, S. Abrate (Ed.), *Impact engineering of composite structures*, Springer, Wien, pp. 193–264, 2011.

[6] G. Belingardi, S. Boria, J. Obradovic, Energy absorbing sacrificial structures made of composite materials for vehicle crash design, *Dynamic Failure of Composite and Sandwich Structures*, Springer, 192:577-609, 2013.

[7] S.Boria, J.Obradovic, G.Belingardi, Experimental and numerical investigations of the impact behaviour of composite frontal crash structures, *Composites: Part B*, 79:20-27, 2015.

[8] D.H.-J.A. Lukaszewicz, "Automotive Composite Structures for Crashworthiness", in *Advanced Composite Materials for Automotive Applications: Structural Integrity and Crashworthiness* (ed A. Elmarakbi), John Wiley & Sons Ltd, pp. 99-127, 2013.

[9] B. Sadasivam, J.G. Cherng, P.K. Mallick, Dynamic response of impact damaged random fiber automotive composites, *Journal of Reinforced Plastics and Composites*, 19:124-136, 2000.

[10] S.J. Rios, R. Arrowood, Impact damage in e-glass/polypropylene compared to e-glass thermoset laminates, 44th International SAMPE Symposium, May 1999.

[11] http://www.pure-composites.com/

[12] H. Han, Stability and crushing behaviors of cylindrical tubes with a cutout, including the mitigation of their local instability using shape memory alloys, Phd Thesis, Dalhousie University, 2006.

[13] J.C. Xaviera, N.M. Garrido, M. Oliviera, J.L. Moraisa, P.P. Camanhoc, F. Pierron, A comparison between the Iosipescu and off-axis shear test methods for the characterization of Pinus Pinaster Ait, *Composites: Part A*, 35, 827-840, 2004.

[14] N.Iosipescu, New accurate procedure for single shear testing of metals, *Journal of Material Science*, 2(3):537-566, 1967.

[15] D.E.Walrath, D.F.Adams, The Iosipescu shear test as applied to composite materials, *Experimental Mechanics*, 23(1):105-110, 1983.

[16] A.-M. Harte, N.A. Fleck and M.F. Ashby, Energy absorption of foam-filled circular tubes with braided composite walls, *European Journal of Mechanics-A/Solids*, 19:31-50, 2000.

[17] G.C. Jacob, J.F. Fellers, S. Simunovic and J.M. Starbuck, Energy absorption in polymer composite materials for automotive crashworthiness, *Journal of Composite Materials*, 36(7):813-850, 2002.
[18] D. Hull, Axial crushing of fibre reinforced composite tubes, *Structural Crashworthiness*, Butterworth and Co Ltd, 1983.
[19] S.P. Timoshenko, J.M.Gere, *Theory of Elastic Stability*, McGraw-Hill Book Company, Inc., 1961.
[20] T. Wierzbicki, W. Abramowicz, The mechanics of deep plastic collapse of thin walled structures, *Structural Failure*, John Wiley & Sons, 1989.
[21] H. Horton, S.C. Bailey, A.M. Edwards, Nonsymmetric buckle patterns in progressive plastic buckling, *Experimental Mechanics*, 6:433-444, 1966.
[22] V. Tvergaard, On the transition from a diamond mode to an axisymmetric mode of collapse in cylindrical shells, *International Journal of Solids Structures*, 19(10):845-856, 1983
[23] N. Jones, Structural impact, *Cambridge University Press*, New York, 1997.
[24] S. Boria, A. Scattina and G. Belingardi, Axial energy absorption of CFRP truncated cones, *Composite Structures*, 130:18-28, 2015.
[25] P.H. Thornton, The crush behavior of pultruded tubes at high strain rate, *Journal of Composite Materials*, 24:594-615, 1990.
[26] P.H. Thornton, Energy absorption in composite structures, *Journal of Composite Materials*, 13:247-262, 1979.
[27] G.L. Farley, Energy absorption of composite materials, *Journal of Composite Materials*, 17:267-279, 1983.
[28] G.L. Farley, The effects of crushing speed on the energy absorption capability of composite tubes, *Journal of Composite Materials*, 25:1314-1329, 1991.
[29] A.G. Mamalis, Y.B. Yuan, G.L. Viegelahn, Collapse of thin wall composite sections subjected to high speed axial loading, *International Journal of Vehicle Design*, 13(5/6):564-579, 1992.
[30] D.W. Schmuesser, L.E. Wickliffe, Impact energy absorption of continuous fiber composite tubes, *Journal of Engineering Material and Technique*, 109:72-77, 1987.
[31] S. Ramakrishna, Energy absorption characteristics of knitted fabric reinforced composite tubes, *Journal of Reinforced Plastics and Composites*, 14:1121-1141, 1995.
[32] D.C. Bannerman, C.M. Kindervater, Crash energy absorption properties of composite structural elements" in *4th International Conference SAMPE European Chapter*, Bordeaux, pp. 155-167, 1984.